Chapter 3

Fabrication of Dual-Stator Axial-Flux Permanent Magnet Synchronous Generator

3.1 Introduction

The Previous chapters discussed the components of the proposed Roof-top Wind Energy Conversion System (RWECS) and the technique of voltage control at variable wind speed and load. In the proposed RWECS model a Dual-Stator Axial-Flux Permanent Magnet Synchronous Generator (DSAF PMSG) has been used as the wind generator.

This chapter discusses the process of design and fabrication of a proof-of-concept DSAF PMSG pre-prototype. Also, incorporating the mechanical provision of displacing one of the stator with respect to the other in the topology has been discussed and implemented.

3.2 Design of Dual-stator Axial-Flux Permanent Magnet Synchronous Generator (DSAF PMSG)

Chapter two elaborates and justifies the choice of DSAF PMSG as a wind generator in the proposed RWECS. Proof-of-concept generators have been manufactured for experimental validation of the proposed wind energy system. It is to be noted that the prototype machine constructed is not based on optimized design and is constructed using material available. The proof-of-concept machine is used to validate the performance of using a mechanically field-weakened PMSG as a variable-speed wind generator operating under high turbulent and intermittent wind conditions. Three machines have been designed and fabricated, and one machine characteristic have been simulated for the necessary experimentations, the design details have been tabulated in Table 3.1. The fabricated generator topology are namely:

1. Topology 1 (T1): 2 phase, 6 pole, 12 slots DSAF PMSG
2. Topology 2 (T2): 3 phase, 4 pole, 18 slots DSAF PMSG
3. Topology 3 (T3): 3 phase, 4 pole, 18 slots coreless DSAF PMSG
4. Topology 4 (T4): A simulated trapezoidal back-emf BLDC generator

3.2.1 Stator design

Stators in the prototypes T1 and T2 use toroidal current transformer cores of Non-grain oriented sheet steel rolled in the form of a pancake, as shown in Fig. 3.1. Slots are made on it using a milling machine. However, in the process the stator lamination has been short circuited and therefore incure eddy current losses. Though, during the experimentations the temperature of the core has not been found high and therefore, the process of slot cutting has been accepted for a proof-of-concept generator fabrication. The T3 prototype

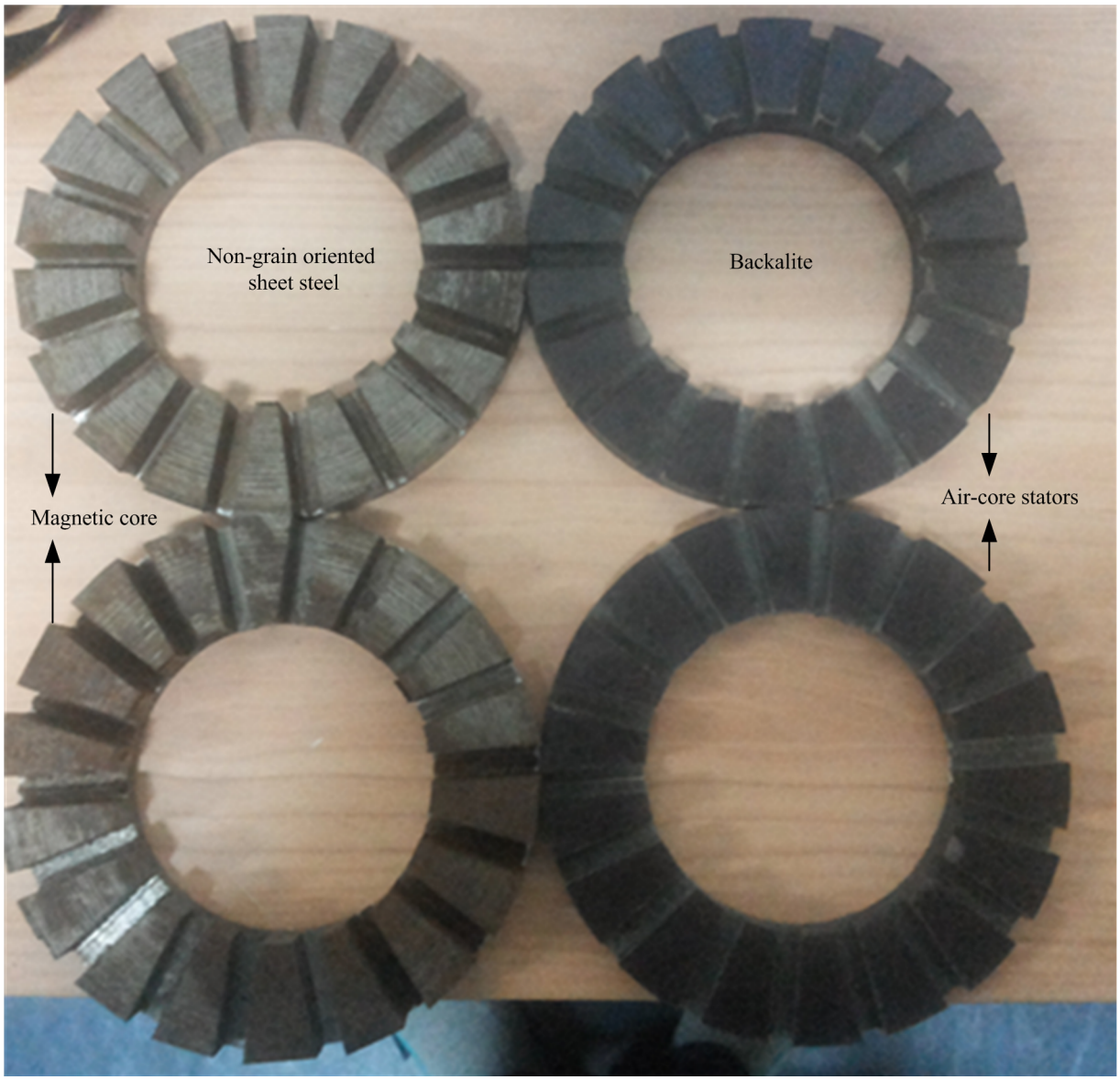

Fig. 3.1 Pancake-shaped stator cores of topology T2 and T3.

uses an air-core stator (made of bakelite, a non-magnetic material), as shown in Fig. 3.1, owing to the advantages such as the absence of cogging torque, perfect-sinusoidal back emf, high efficiency, and reduced manufacturing cost [54].

The outer and inner stator diameter in topology T1 has been decided based on the dimension of imported magnet available in the lab. The design parameters are listed in Table 3.1. The aspect ratio for T1 is 2.66. In topology, T2 and T3 the aspect ratio in an axial flux machine is taken as to be equal to ideal value of $\sqrt{3}$ [50]. The ideal aspect ratio is based on ease of doing three-phase distributed winding in the stator. Topology T1 uses concentrated tooth winding. The high aspect ratio in topology T1 increases the active length of the winding. However, the per unit r_g of the winding increases due to low induced emf at stator inner radius. Moreover, the tooth coil resulted in a short pitch factor of 0.707. Therefore, topologies T2 and T3 use distributed windings with short pitch factor 0.86. Table 3.1 tabulates the design parameters for all the three topologies.

Winding details: Topology T1 consists of 12 number of semi-closed circular slots in each stator. The number of stator slots has been decided to ensure the proper mechanical strength of the teeth at the inner radius of the stator. Finally, the stator is wounded to create a 2 phase, six pole slot-by-slot winding with SPP = 1. Fig. 3.2 shows pictures of the wounded stators used in the fabricated machine.

However, the back emf characteristic of the machine during the experimentation is high peak sinusoidal, as shown in 6.1 (a). The machine characteristics are due to the use of magnet pole to pole pitch ratio as to be unity, as shown in Fig. 3.14 (b), and thus, the presence of a small interpolar region. Fig. 3.3 shows the slot-vector diagram of the winding.

Table 3.2 and Fig. 3.4 provides the winding details. Topology T2 and T3 consist of 18 semi-closed rectangular shaped slots with distributed windings. The windings are connected to develop a 3 phase, 4 poles, double layer distributed winding with SPP =

Table 3.1 Design parameters of Topology T1, T2, and T3 [134–136].

Parameters	**Specifications**		
	Topology T1	**Topology T2**	**Topology T3**
No. of phases	2	3	3
Output phase voltage	26.5 V per phase per stator	24 V per phase per stator	15 V per phase per stator
Power	100 W	144 W	90 W
Rated Speed	1000 rpm	1000 rpm	1000 rpm
No. of poles	6	4	4
No. of slots	12	18	18
Slot dimension	Circular semi-closed slots with 12 mm dia Wedge 2 mm	Rectangular slots 8 mm wide and 14 mm depth Wedge 2 mm	Rectangular slots 8 mm wide and 10 mm depth Wedge 2 mm
Slot opening	2 mm	2 mm	Not applicable
Inner radius of stator	35 mm	48 mm	48 mm
Outer radius of stator	80 mm	80 mm	80 mm
No. of turns per coil	45	45	22
Winding type	Concentrated double-layer tooth winding	Double layer distributed	Double layer distributed
NdFeB magnet	N35	N35H	N35 H
Magnet operating temperature	80_oC	200_oC	200_oC
Magnet shape	Arc shape	Arc shape	Arc shape
Magnet dimensions	76.15 mm outer diameter 36.75 mm inner diameter	96 mm inner dia 160 mm outer dia	80 mm outer radius 48 mm inner radius
Magnet arc-length	60^o mech degrees	70^o mech degrees	70^o mech degrees
Magnet width	3 mm	3 mm	3 mm
Residual flux density	1.170 T	1.170 T	1.170 T
Air-gap clearance	5.5 mm	5 mm	1 mm

Table 3.2 Winding detail for Topology T1 with 2-phase, 6 pole concentrated tooth winding.

Slot no.	1	2	3	4	5	6	7	8	9	10	11	12
Upper Layer	+a	+b	-a	-b	+a	+b	-a	-b	+a	+b	-a	-b
Bottom Layer	+b	-a	-b	+a	+b	-a	-b	+a	+b	-a	-b	+a

Fig. 3.2 Stators with tooth windings in topology T1.

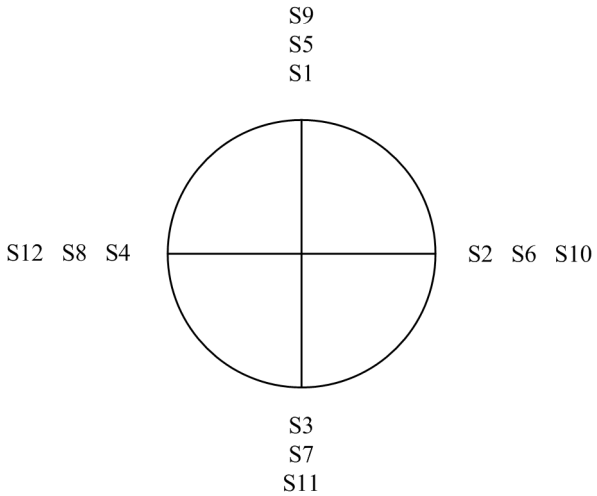

Fig. 3.3 Slot-vector diagram of 12 slots, 2 phase, 6 pole concentrated tooth winding.

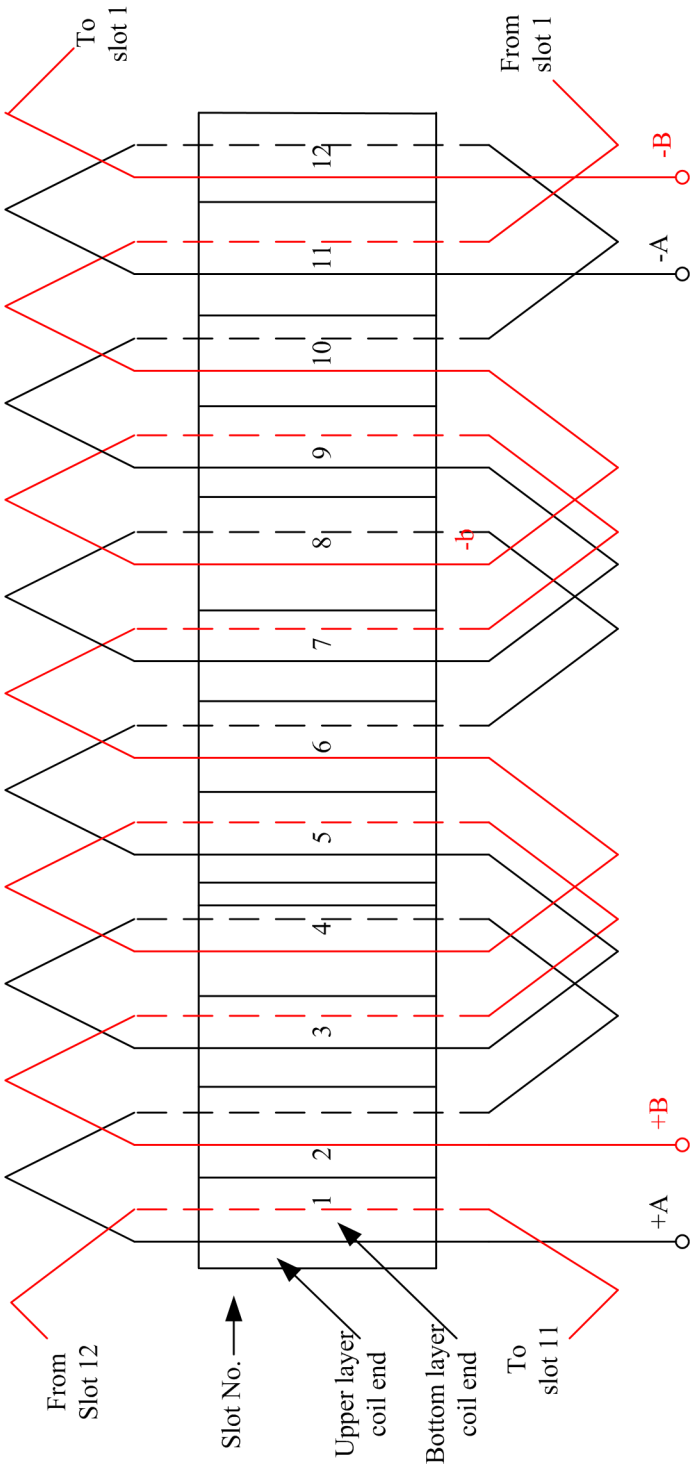

Fig. 3.4 Winding layout of 12 slots, 2 phase, 6 poles, double layer concentrated tooth winding.

Table 3.3 Winding details of 18 slot, 3 phase, 4 poles, double layer distributed winding.

Slot no.	1	2	3	4	5	6	7	8	9	10	11	12	13	14	15	16	17	18
Upper Layer	+a	+b	+b	+b	+c	+c	+c	+a	+a	+a	+b	+b	+b	+c	+c	+c	+a	+a
Bottom Layer	-c	-c	-c	-a	-a	-a	-b	-b	-b	-c	-c	-c	-a	-a	-a	-b	-b	-b

1.5. Fig. 3.5 and 3.6 show the pictures of the wounded stator for topology T2 and T3, respectively. The only difference between the stators of topology T2 and T3 is in the depth of the slots owing to the different mechanical strength of the core materials. Fig. 3.7 shows the slot vector diagram of the 18 slots, 3 phase 4 pole winding. Further, Table 3.3 provides winding details and Fig. 3.8 shows the winding layout. However, due to the selection of a distributed winding with 4 poles in 18 slots, the short pitch factor of the winding reduces to 0.86, and the manufacturing cost of the winding increases.

Tooth windings (most suitable in axial-flux machine) can also generate sinusoidal flux density in air-gap but for specific slot-pole combinations [137]. Therefore, due to the lack of magnets with appropriate dimensions, it was decided to go with conventional distributed winding for T2 and T3 topologies.

As per the topology, two stators with the same dimensions and winding were fabricated. Further, the applied MFW technique requires an angular shift of one of the stators (Rotatable stator (RS)) with respect to the other stator (stationary stator (SS)). Therefore, SS fixes to the experimental platform, and RS attaches to a movable mechanical actuator. Section 4.2.3 provides the details of the system. Subsequently, windings on both stators connect in star network, and respective phases on both stators connect in series as shown in Fig. 3.9. Thus, the output voltage of the generator is the phasor sum of voltages on both stator windings. Fig. 3.10 (a) shows the phasor diagram at stator displacement angle = 0^o electrical and Fig. 3.10 (b) shows the phasor diagram at stator displacement angle = ϕ^o electrical. Mathematically, the generator output voltage and magnitude are represented by Eq. 3.1 and 3.2 respectively.

Fig. 3.5 Stators with distributed windings in topology T2.

Fig. 3.6 Stators with distributed windings in topology T3.

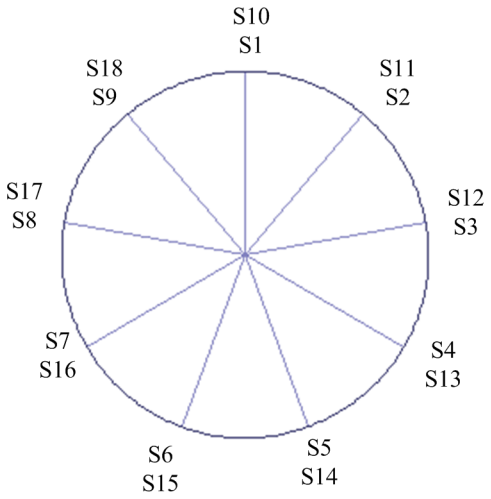

Fig. 3.7 Slot-vector diagram of 18 slots, 3 phase, 4 poles, double layer distributed winding.

$$V_g = V_{SS} + V_{RS}\angle\phi \tag{3.1}$$

$$\left|V_g\right| = V_0 cos(\frac{\phi}{2}) \tag{3.2}$$

V_g is the generator output phase voltage, V_{RS} and V_{SS} are the induced phase voltages in RS and SS windings respectively, and ϕ is phase displacement between V_{RS} and V_{SS}, and also, defined as stator displacement angle (SDA) of RS with respect to SS (in electrical angle). Assuming V_{RS} and V_{SS} of the same magnitude and thus, taken as to be equal to V_o.

Fig. 3.11 shows a simulated plot of V_g against SDA based on Eq. 3.1. At $SDA = 0^o$ electrical (both stators aligned), the generated voltage is one pu, and at $SDA = 180^o$ electrical (One of the stators displaced by one pole pitch with respect to the other), the generated voltage is zero. The results have been validated experimentally on a proof-of-concept DSAF PMSG.

Fig. 3.12 shows the variations in generator output voltage as per the SDA in topology T1. The generator voltage decreases as per the stator displacement angle. However, the generator voltage is not zero at $SDA = 60^o$ mechanical (equivalent to 180^o electrical for

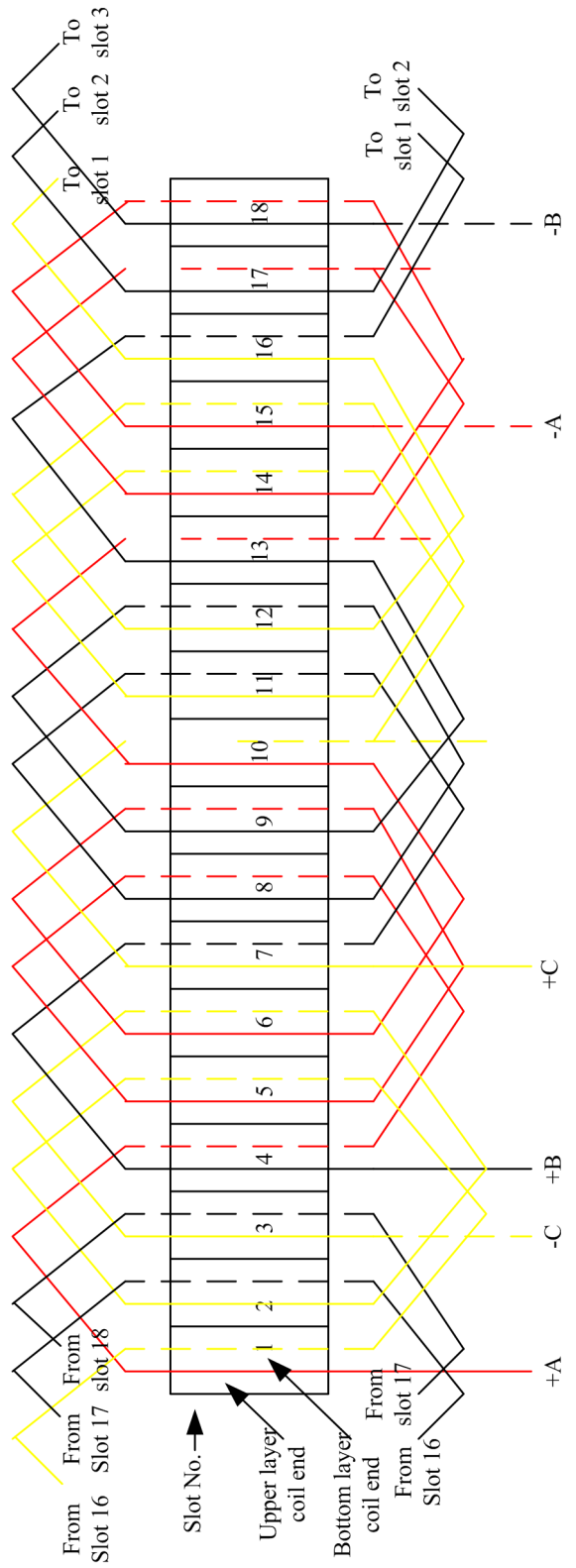

Fig. 3.8 Winding layout of 18 slots, 3 phase, 4 poles, double layer distributed winding.

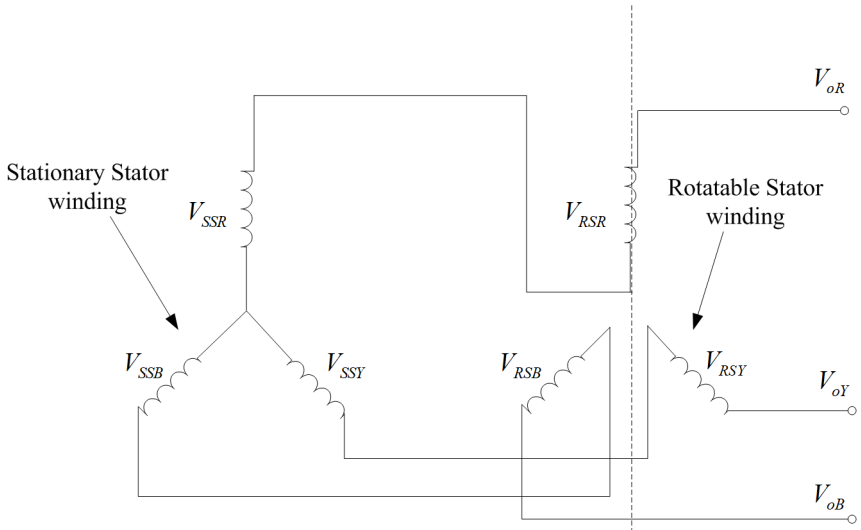

(a) Interconnection of Stationary Stator and Rotatable Stator windings with stator displacement angle $\phi = 0^o$ electrical

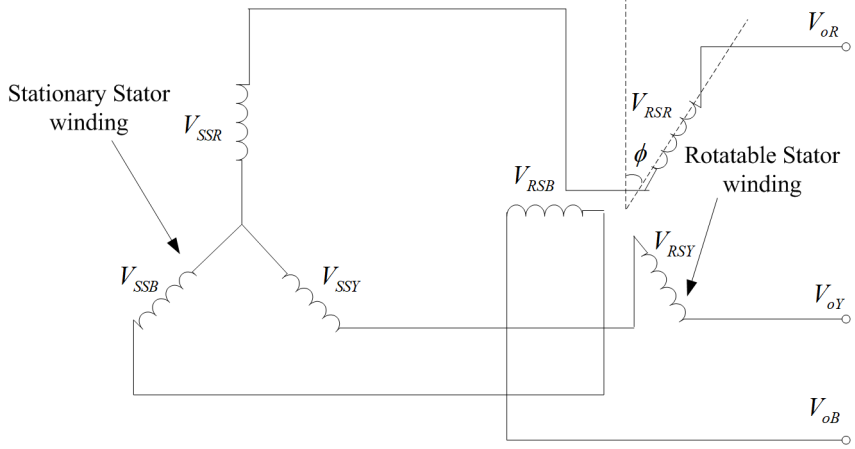

(b) Interconnection of Stationary Stator and Rotatable Stator winding with stator displacement angle ϕ^o electrical

Fig. 3.9 Interconnections of Stationary Stator and Rotatable Stator windings.

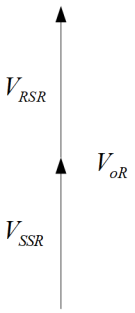

(a) Phasor Diagram of Stationary Stator and Rotatable stator windings with stator displacement angle $\phi = 0^o$ electrical

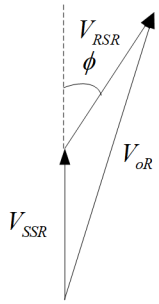

(b) Phasor Diagram of Stationary Stator and Rotatable Stator windings with stator displacement angle ϕ^o electrical

Fig. 3.10 Phasor diagrams of Stationary Stator and Rotatable Stator windings.

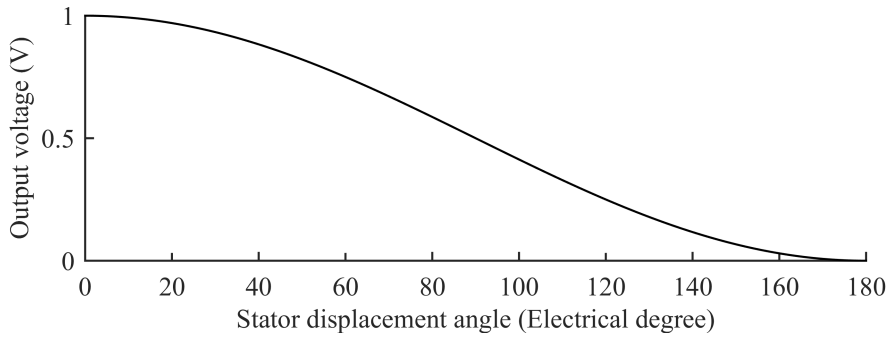

Fig. 3.11 Plot of variation in generator output voltage (rms) as per stator displacement angle.

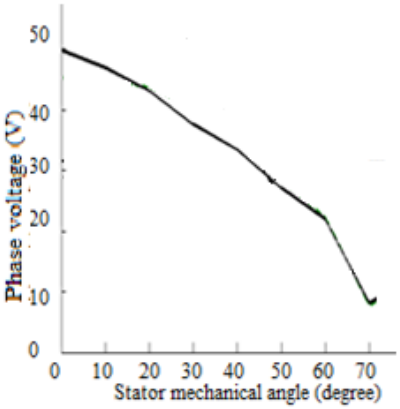

Fig. 3.12 Variations in Generator phase voltage (rms) against stator displacement angle (mechanical degree) for a six pole generator at 1000 rpm rotor speed.

six pole machine) due to unequal voltage induced in the RS and SS winding. The unequal voltages are due to the dissimilar air-gaps due to the mechanical tolerance at both sides of the rotor in the fabricated generator.

3.2.2 Rotor design

The proof-of-concept machine has one disc-shaped rotor, with permanent magnets pasted on both sides, sandwiched between two pancake-shaped stators, as shown in Fig. 3.13. The magnets are axially magnetized and pasted on the rotor in N-S fashion, as shown in Fig. 3.13. The magnetic flux from the PM passes the rotor axially. Therefore, the thickness of the rotor has been chosen as 6 mm, to have sufficient enough mechanical strength to bear axial-forces between the PMs and the magnetic cores. The rotor is made

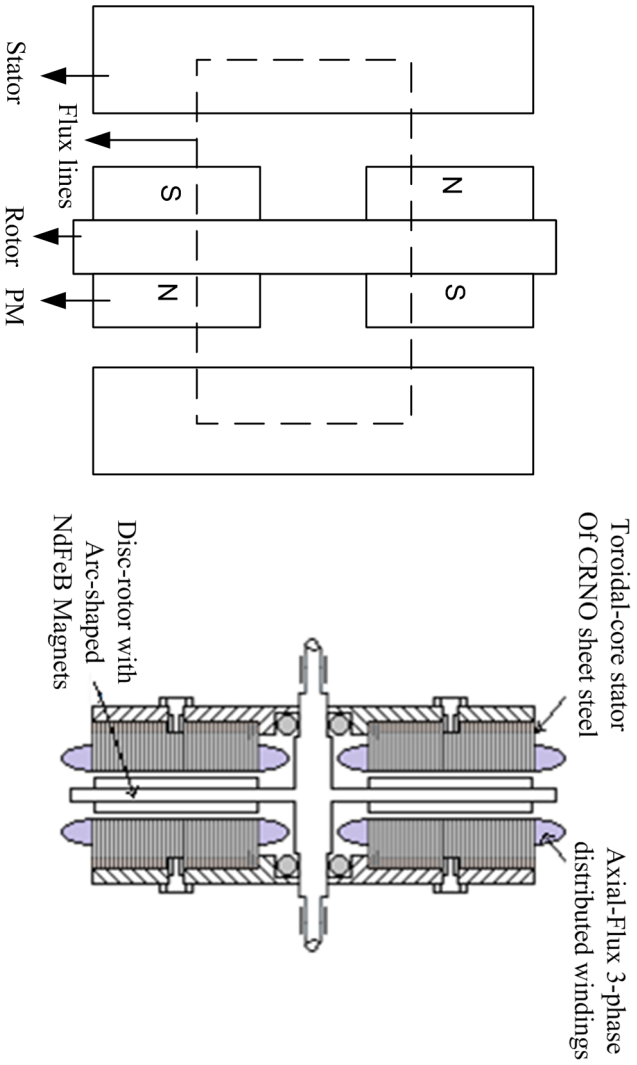

Fig. 3.13 Flux path in the top-view of the DSAF PMSG.

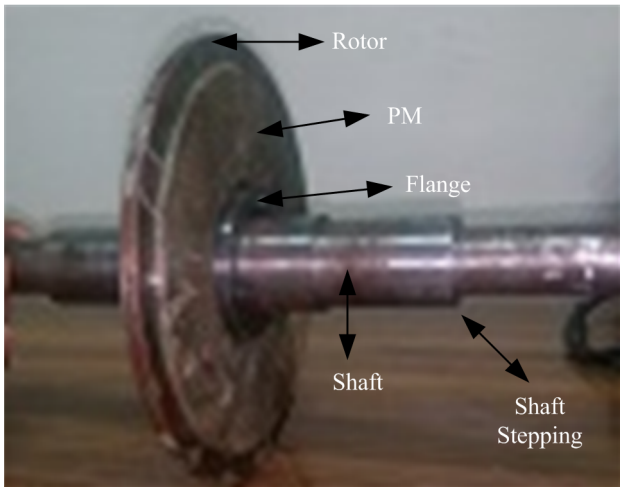

(a) Rotor with flange support.

(b) Rotor with PM .

Fig. 3.14 Rotor fitted on the shaft through flange support and magnets pasted on both sides of the rotor surface.

of a solid mild-steel plate and machined into disc-shape using lathe-machine. Owing to the experimental nature of the prototype, the rotor of the machine is detachable from the shaft. The rotor attaches to a flange on the shaft using bolts so that another rotor with a different set of magnets could replace the same, making the system modular. Fig. 3.14 (a) shows the rotor attached to the shaft through a flange.

Two sets of rotors were used in the experimentation. One rotor consisted of six poles on both sides with pole arc to pole pitch ratio to be unity, as shown in Fig. 3.14b and another rotor consisted of four poles on both sides with pole arc to pole pitch ration to be 0.77 (not shown in the figure).

3.2.3 Assembly of the machine

As per the principle of MFW to be implemented in the DSAF PMSG, a provision is provided to displace the RS with respect to the SS angularly. Therefore, the stators were attached to a potting system through bolts, as shown in Fig. 3.15. Subsequently, a ball bearing is press-fit into the potting. Finally, the pottings rest on the collars of the shaft from each side of the rotor, as shown in the Fig. 3.16.

Fig. 3.15 Variations in Generator phase voltage against stator displacement angle (Stator bolted to a potting arrangement).

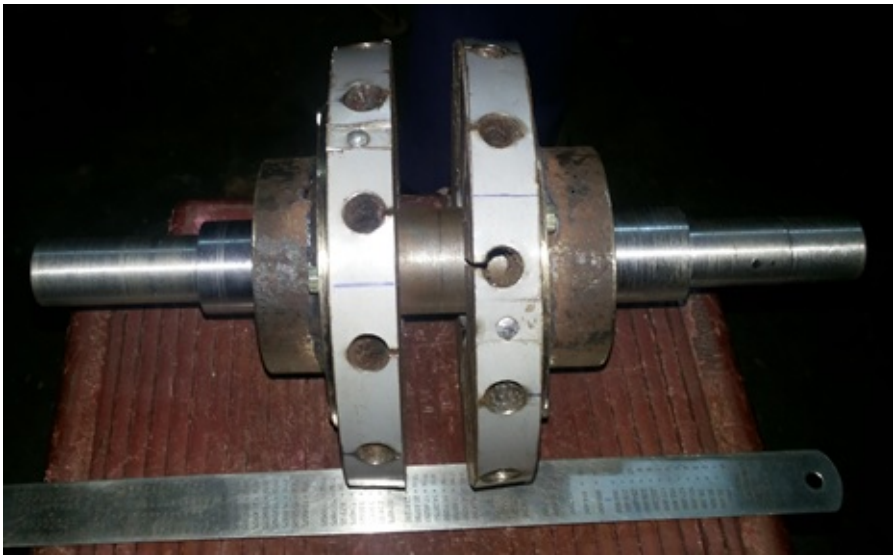

Fig. 3.16 Stator-potting arrangement resting on the stepping on the shaft through ball-bearing.

The potting-stator arrangement makes the stator free to rotate on the shaft. To rotate RS with respect to SS, SS potting is fixed to the platform of the setup, and RS potting is attached to a worm wheel gear, as shown in the Fig. 3.17. Subsequently, the worm wheel gear is attached to a stepper motor (specified as a mechanical actuator in the figure) to rotate the RS in the required steps.

3.3 Conclusion

This chapter discusses the process followed in the design and fabrication of a dual-stator axial-flux permanent magnet synchronous generator. Three proof-of-concept PMSG topologies have been fabricated and one BLDC topology has been simulated. Mechanical provision of rotating one of the stator with respect to another in the topology has been achieved by fixing the stationary stator with the setup platform and the rotatable stator to a stepper motor through a worm-wheel gear. In the fabricated generator field-weakening has achieved by rotating the rotatable stator with respect to the stationary stator.

The next chapter discusses the experimental hardware setup. The experimental hardware setup is designed to do experimentations on the proposed RWECS to validate the principle of concept of this thesis.

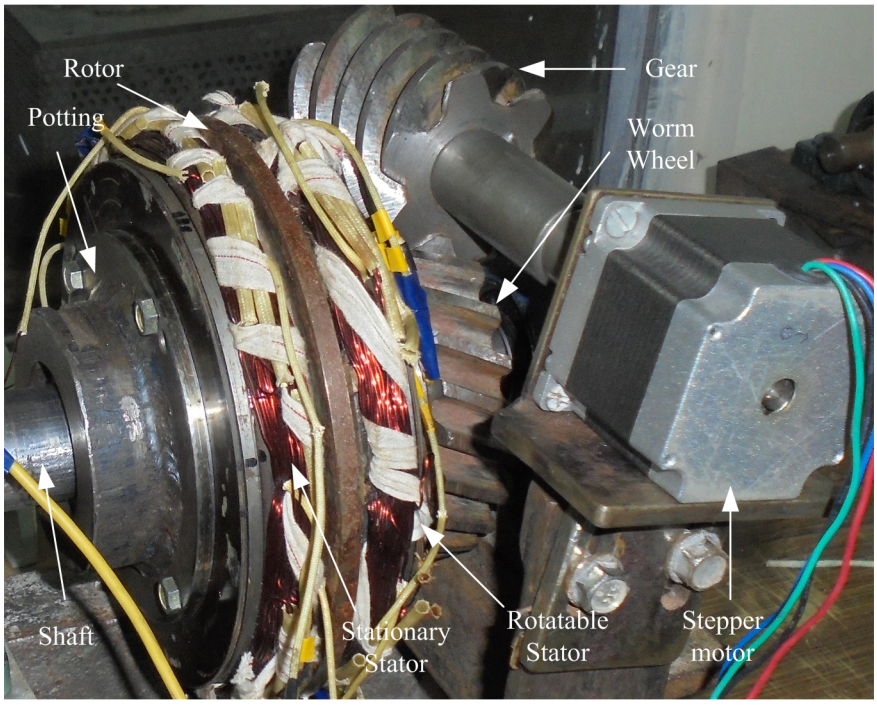

(a) Side-view of the generator

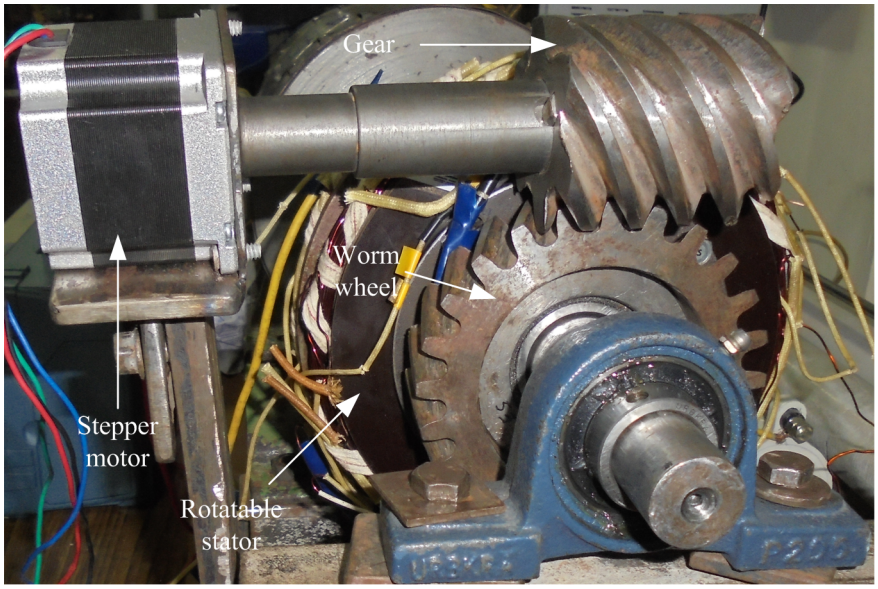

(b) Front-view of the generator showing the worm-wheel gear arrangement .

Fig. 3.17 Assembly of the dual-stator axial-flux permanent magnet synchronous generator with provision of displacing one of the stator with respect to the other stator.